



UNICA

UNIVERSITÀ
DEGLI STUDI
DI CAGLIARI



Università di Cagliari

UNICA IRIS Institutional Research Information System

This is the Author's manuscript version of the following contribution:

Intini, C. *et al.* 3D-printed chitosan-based scaffolds: An in vitro study of human skin cell growth and an in-vivo wound healing evaluation in experimental diabetes in rats. *Carbohydr. Polym.* **199**, (2018).

The publisher's version is available at:


<https://doi.org/10.1016/j.carbpol.2018.07.057>

When citing, please refer to the published version.

This full text was downloaded from UNICA IRIS <https://iris.unica.it/>

3D-printed chitosan-based scaffolds: an *in vitro* study of human skin cell growth and an *in-vivo* wound healing evaluation in experimental diabetes in rats

Claudio Intini^{1,3}, Lisa Elviri^{1*}, Jaydee Cabral², Sonya Mros³, Carlo Bergonzi¹, Annalisa Bianchera¹,
Lisa Flammini¹, Paolo Govoni⁴, Elisabetta Barocelli¹, Ruggero Bettini¹, Michelle McConnell M³

¹Food and Drug Department, University of Parma, Parco Area delle Scienze 27/A, 43124, Parma, Italy. 

²Department of Chemistry, University of Otago, Dunedin 9054, New Zealand.

³Department of Microbiology & Immunology, University of Otago, Dunedin 9054, New Zealand.

⁴ Department of Medicine and Surgery, University of Parma, Parma, 43124, Parma, Italy.

Lisa Elviri

¹Food and Drug Department, University of Parma, Parco Area delle Scienze 27/A, 43124, Parma, Italy.

* Corresponding Author

E-mail: lisa.elviri@unipr.it

Abstract

The progress seen in biomaterials manufacturing strategies and 3D printing technology shows a fundamental driving force for the development of innovative therapies in the tissue engineering field. In this paper, the fabrication of porous 3D printed chitosan (CH)-based scaffolds for skin tissue regeneration and their behavior in terms of biocompatibility, cytocompatibility and toxicity toward two different skin associated human cell lines of fibroblast (Nhdf) and keratinocyte (HaCaT), are presented and discussed. To this purpose, two different types (i.e. with or without a CH film at the base) of CH-based scaffolds were realized using a versatile and cost-effective extrusion-based 3D printing process. Neutral Red stain and MTT results of 3D cell cultures achieved after 20 and 35 days of incubation showed significant *in vitro* qualitative and quantitative cell growth. Cell adhesion and colonization were also confirmed by scanning electron microphotographs. The best results were obtained after 35 days on 3D scaffold printed with the film at the bottom when the Nhdf and HaCaT cells, seeded together, filled the scaffolds. Moreover, an early skin-like layer consisting of a mass of fibroblast and keratinocyte cells growing together was observed, demonstrating an attractive potential for applications in skin tissue regeneration. Finally, the efficacy of 3D printed scaffolds in wound healing was tested on streptozotocin-induced diabetic rats using histological methods. The results demonstrate that 3D printed scaffolds improve the quality of the restored tissue with respect to traditional chitosan scaffolds or the spontaneous healing. 3D technology is demonstrated to generate improved scaffolds for therapeutic applications in an automatized manner.

Keywords: 3D printing, chitosan scaffold, chitosan biocompatibility, fibroblast and keratinocyte cells, skin tissue engineering.

INTRODUCTION

Tissue engineering is a promising field of regenerative medicine that relies on the interaction of three main elements: a supporting material, growth factors, and cells to develop a biological substitute for the replacement, restoration or regeneration of damaged tissues and organs. [1] The challenge of this matter is to mimic what happens in nature. Attempts (are being made) have been made to engineer *in vitro* various tissues and organs. To date, the highest rates of success have been achieved in the areas of skin, [2] bladder, [3] airway, [4] and bone, [5, 6] where tissue-engineered constructs have been successfully used in patients. [7-9]

Focusing attention on skin tissue engineering, the production of extra-cellular matrix (ECM) plays a pivotal role in the regeneration process, driving cell proliferation, differentiation and maturation. Furthermore, ECM provides characteristics of storage and delivery of growth factors and cytokines and it supplies structural integrity and scaffolding features as *substratum* for glycosaminoglycans such as, hyaluronic acid (HA) and collagens, naturally secreted by recruited cells during initial phases of regeneration. [10]

A relevant task of skin tissue engineering is thus focused towards the bio-fabrication and use of porous three-dimensional (3D) scaffolds [1] as appropriate environments for cell colonization and proliferation, thereby enabling the production of ECM and the reconstruction of complex tissues.

Among the different scaffold preparation processes, [11-13] 3D printing and bioprinting are innovative technologies drawing tremendous attention from both academia and industry for their potential applications in various fields, including regenerative medicine and pharmaceutical drug delivery. Biomaterials, biomolecules and/or cells are patterned by 3D advanced additive manufacturing technologies to create scaffolds with arbitrary geometries and heterogeneous material properties, which can mimic the complexity of native tissues. [14] Although 3D bioprinting presents revolutionary capabilities, the design and fabrication of 3D devices are critical. One of the key points is that scaffold constructs should address the needs for architecture design at the macro, micro, and nano level involved in structural cell-matrix interactions and nutrient transport. [15, 16] Current 3D printing techniques (i.e. extrusion printing, laser printing, droplet printing), are feasible to make

accurate and rapid fabrication of pre-designed structures with several natural (i.e. alginate, chitosan, collagen etc.) and synthetic polymers (polylactide, polyethylene glycol, etc.) with resolution ranging from 20 μm for laser techniques to 200-300 μm for the droplet and extrusion printing, respectively. [17]

In the present work, an innovative extrusion-based 3D printing technique has been used for the preparation of novel 3D chitosan scaffolds presenting controlled and reproducible macro- and micro-structure to be applied in the regenerative skin tissue field. [18,19] This manufacturing approach combines the freeze-gelation method described by Elviri *et al.* (2014) [20] alongside an advantageous modification of the chitosan solution with raffinose [18] with the technical advantages of 3D printing. Chitosan (CH) is a natural polysaccharide derived from the alkaline N-deacetylation of chitin, the main structural component of the crustacean exoskeleton. [21] When the number of N-acetylglucosamine units is higher than 50%, the biopolymer is referred to as chitin. Conversely, when the number of N-glucosamine units is higher, the term chitosan is used. Chitosan has the potential to be biocompatible, does not elicit adverse reactions in contact with human cells, is not allergenic and is cheap. [22, 23] It can be molded into a variety of shapes, can be degraded by ubiquitous enzymes in the human body, and oligomeric products from degradation can activate macrophages and stimulate synthesis of hyaluronic acid. [24, 25] Moreover, chitosan and chitin present haemostatic action which can be exploited to enhance healing. [26] For these reasons, chitosan is one of the most investigated biomaterials for tissue engineering and bio-fabrication. In the last decade, several chitosan-based biomedical applications including wound dressing, [27, 28] drug delivery, [29,30] and space filling implants [31,32] have been successfully achieved. Presently, many chitosan-based medical devices are in clinical trials with the highest applications in bone, cartilage and skin tissue regeneration. [33] Although plenty of chitosan scaffolds have been studied in different cell cultures, the potential of 3D printed constructs on cell behavior is still under investigation as this is an important feature to be investigated before any *in-vivo* application.

In light of applications for dermal chronic wound treatments, in the present paper, the biocompatibility, cytocompatibility and toxicity of 3D printed chitosan scaffolds towards human skin cell lines were investigated. In our previously published paper, [19] the effect of a simple 3D printed architecture with 400 μm opening was demonstrated to significantly improve human fibroblasts adhesion and proliferation with respect to scaffolds prepared by casting. In order to improve the understanding about the role of the third dimension on the accurate improvement of *in vitro* results, two different 3D scaffolds with 200 μm inter-filament opening were prepared (i.e. 3D printed scaffolds with or without the film of chitosan at the base) and individual and co-culture of fibroblast and keratinocyte cells were monitored.

In addition, in order to obtain evidence about the 3D scaffolds properties to improve tissue regeneration, these 3D scaffolds were assessed *in vivo* in a context mimicking a clinical feature such as the model of wound healing in streptozotocin-induced diabetic rats.

The results obtained were reported and discussed.

MATERIALS AND METHODS

Materials

Chitosan ChitoClear® Fg90 TM4030 (CAS 9012-76-4, deacetylation degree 75%; molecular weight by gel permeation chromatography 50-60 kDa; allergen free, water insoluble, soluble in acid media) was from PRIMEX Ehf (Siglufjordur, Iceland).

Acetic acid 99.8% v/v, dimethyl sulfoxide (DMSO) and potassium hydroxide were from J.T. Baker (Deventer, Netherland). Water was purified (0.055 $\mu\text{S}/\text{cm}$, TOC 1ppb) with a Purelab pulse + Flex ultra-pure water system (Elga Veolia, Milan, Italy).

Neutral Red stain solution and MTT (3-(4,5-dimethylthiazol-2-yl)-2,5-diphenyl tetrazolium bromide) reagent were purchased from Sigma-Aldrich (St. Louis, MO, USA). MTT reagent was dissolved in water and stocked at concentration of 5 mg/mL; final concentration used was 1 mg/mL.

3D Printer

A 3D home-made low temperature manufacturing system, built by combining Peltier cells and liquid/air exchangers, was used at the laboratory scale through the insertion of bespoke modules in the structure of a commercial Fuse Deposition Manufacturing (FDM) 3D printer. FDM architecture is based on three Cartesian axes, two of which enliven the printing plate in x and y direction on the horizontal plane, while the z-axis determines the progressive lifting of the extrusion nozzle. The design of scaffold shapes was directly described by the geometric primitives of the axis control, without need of translating them through general purpose programs for the transformation of the 3D CAD model in a mesh to be subjected to slicing.

3D Chitosan scaffold fabrication

All 3D chitosan scaffolds were constructed from a chitosan solution (6% w/v) in acetic acid 2% (v/v) containing D-(+) raffinose pentahydrate at a final concentration of 290 mM. [18] The resulted chitosan solution was treated in an ultrasonic bath for eliminating possible bubbles and clusters that could cause processing problems, such as nozzle clogging during 3D printing process. Thereafter, the solution was used to fill the 3D printer's cartridge, which was then assembled on the whole equipment. The 3D printer was constituted by a mechanical apparatus that could be moved along the three dimensions on axes-x,-y,-z, an extrusion system, composed in turn, by a syringe (volume 5mL) and a needle (26 gauge), that could be assembled and disassembled, and a mobile plate on which the solution was extruded and cooled at -14 °C with a series of Peltier cells. Several 3D chitosan scaffolds were printed following the extrusion-based 3D printing process. The 3D matrices were characterized from a projected area of 1 cm², a thickness of the first layer of about 0.3 mm and a thickness of the other layers of about 0.2 mm for a total of 2.1 mm, and an opening of the network of 200 µm. Right after the 3D printing process, the scaffolds were gelled in potassium hydroxide KOH 8% (w/v) for 10 minutes and then stored in phosphate buffer saline PBS. This last passage was necessary to

increase the material rigidity for filament shape retention. A further, 3D chitosan structure was produced which consisted of a compact chitosan film at the base to the previously realized scaffolds. The purpose of this film was to occlude the lower base of scaffold to improve the cell growth on it by keeping the cells inside. In detail, starting from the above-described chitosan solution, the film was casted and uniformly spread on the plate of the 3D printer using a roll film, before the printing process. After that, the 3D scaffold was printed above the film following the already mentioned procedures.

Mechanical resistance analysis

The mechanical resistance of scaffolds obtained was calculated on 20-layers scaffolds having size of 5 cm x 1.5 cm. Thickness was determined as a mean of six measurements of the scaffold performed with a digital micrometer (Mitutoyo, Japan). Each scaffold was fixed on a tensile tester (AG M1 Acquati, Italy) loaded with a 5 DaN cell. Force and time signals were digitalized by means of a PowerLab 400 board and recorded with Scope 3.5 software. Elongation at break and Young's modulus were determined from the relevant stress-strain curves.

Cell cultures

Normal dermal human fibroblast cells (Nhdf cells) and aneuploid immortal keratinocyte cells (HaCaT cells) obtained from American Type Culture Collection (ATCC®, Manassas, VA, USA) were used for *in vitro* tests.

Frozen stocks of these human cells at 1×10^6 cells/mL were initially put in 250 mL flasks, and sub-cultured in 750 mL flasks. Both cells were passaged in 750 mL flasks containing complete Dulbecco Modified Eagle Medium (DMEM, Gibco™, Thermo Fisher Scientific, Waltham, MA, USA) supplemented with 10% Fetal Bovine Serum (FBS, Gibco™, Thermo Fisher Scientific, Waltham, MA, USA) and 1% Penicillin and Streptomycin (PenStrep, Sigma-Aldrich, Saint Louis, MO, USA). Cells were incubated at 37 °C, 5% CO₂ in a cell culture incubator and were sub-cultured at 70%

confluence.

3D Cell cultures

Fibroblast (Nhdf) and keratinocyte (HaCaT) cells were seeded individually at a concentration of 1×10^5 cells/mL on 3D chitosan scaffolds with or without the film of chitosan at the base; scaffolds were previous sterilized for 24 hours in 70% v/v ethanol. Each scaffold was inserted and seeded in a single well of a 12 or 24-well plate (Falcon® 12 or 24 Well Clear Flat Bottom TC-Treated Multiwell Cell Culture Plate, Corning®, New York, USA). Each plate's well was then filled with 1 mL or 2 mL of complete culture medium (DMEM, 10% FBS and 1% P/S) relative to whether the 12 or 24-well plate was used. The media was changed every 2 days in the first week of culture and every day in the remaining time of the experiment. When the cells were seeded together, Nhdf cells were added first on the scaffold in the specific well at 1×10^5 cells/mL concentration. Then, after one week, the culture medium was renewed and HaCaT cells at 2×10^5 cells/mL concentration were added. All 3D cell cultures were maintained in a 5% CO₂ incubator at 37 °C.

Neutral red assay

The Neutral Red assay [34] was used to provide a qualitative estimation on the presence of viable cells on 3D chitosan scaffolds at defined time points. The medium was removed from the 3D cell cultures to be washed with PBS. Thereafter, the 3D chitosan scaffolds were placed in a fresh plate in order to stain the cells growing on the scaffolds. The Neutral Red assay was performed by adding 150 µL of Neutral Red solution (0.5% w/v) for each well. The cultures were left in staining solution for 5 minutes at room temperature. They were washed two times carefully and gently with PBS for 5 minutes each and at the end, 150 µL of PBS were added to each culture/well before visualization. The results were observed under the transmitted light of an inverted microscope (Leica DM IL, Bio-Strategy Ltd., Albany, New Zealand). Each completed assay corresponded to one time point of analysis.

MTT assay

Fibroblast (Nhdf) and keratinocyte (HaCaT) cells seeded together on 3D chitosan scaffolds with and without the film of chitosan at the base were analyzed after 2, 13, 20 and 35 days by means of a MTT cell viability assay [35]. Using this method, the total number of cells that were situated on the scaffold and on the plastic at the bottom of the well were quantitated. In detail, at each time point, the medium was removed from the cultures, the 3D scaffolds were washed once with PBS and inserted in a fresh well plate to be analyzed. 1 mL of MTT reagent solution at concentration of 1 mg/mL dissolved in PBS was added to each well. The 12 or 24 well-plate was then covered with aluminum foil as MTT is light sensitive, and was incubated at 37°C, 5% CO₂ for 1 hour. MTT reagent was also added to the original wells where the 3D chitosan scaffolds came from in order to measure the cells grown on the bottom plastic surface of the well. Then, MTT solution was replaced by pipetting 1 mL of acidified isopropanol, prepared by adding hydrochloric acid (37% w/v) to isopropanol (1:1000 volume ratio) into each well. Finally, the plate was placed on a rotating platform for 10 minutes at 100 rotation per minute to ensure complete solubilization of the formed blue formazan crystals. The absorbance values were read at 570 nm using a Varioskan Flash Multimode Reader (Thermo Fisher Scientific, Waltham, MA, USA). Different dilutions of the samples, using acidified isopropanol solution, could be required depending on the viable cell numbers expected. Each completed assay corresponded to one time point of analysis. Moreover, this assay was also performed using two control groups, the 3D chitosan scaffolds only without cells, and cells only without scaffolds.

Scanning electron microscope (SEM) analysis

Fibroblast and keratinocyte cells were seeded alone and together on both types of 3D chitosan scaffolds. After 20 and 35 days, the cultures were fixed in 2.5% glutaraldehyde and in 0.1M cacodylate buffer for a total of 2 hours. They were then washed 3 times with PBS, post-fixed in 1% osmium tetroxide, and in PBS for 1 hour. Then the samples were dehydrated in 30%, 50%, 70%,

80%, 95%, 100% v/v (the latter for 3 times) ethanol for 10 min each step and the Critical Point Drying CPD (Bal-Tec AG, Balzers, Liechtenstein) was performed at 31°C. Then, the 3D chitosan scaffolds were mounted on 12.5 mm aluminum stubs using double sided carbon tape and carbon paste and coated with 10 nm of gold palladium for SEM viewing. 3D cell cultures were visualized with a scanning electron microscope (Zeiss Sigma VP, Carl Zeiss, Oberkochen, Germany), at several magnification values, EHT 1.00 kV and analyzed by Image J software (NIH, Bethesda USA).

Streptozotocin-induced diabetic model in rats

Research protocols were approved by the Italian Ministry of Health (D.Lgs 26/2014 ex D.Lgs.116/92) and the experiments were carried out in compliance with the Guide for the Care and Use of Laboratory Animals published by the US National Institutes of Health.

Adult female Wistar rats, weighing 250 to 350g, were used in this study. The animals were kept in environmentally controlled rooms ($22^{\circ} \pm 2^{\circ}\text{C}$, humidity $55 \pm 10\%$, 12 h light and dark cycle). The animals were allowed to take normal rat feed (reference laboratory food pellets (4RF21, Mucedola Srl, Settimo Milanese, Italy) and drinking water without restriction.

After an overnight fast, all animals (n=25) received an intraperitoneal injection of streptozotocin (50mg/kg; Sigma-Aldrich). Streptozotocin induces diabetes within 3 days by destroying the pancreatic β -cells; therefore 72h after injection, blood glucose was measured in overnight fasting animals. STZ-treated rats with whole-blood glucose levels higher than 250mg/dL were considered diabetic and used in the study. Fasting blood glucose was determined every 7 days throughout the experimental time to confirm the diabetic state, that leads to a delay in the time of wound healing with respect to physiological conditions. Rats were kept in cages individually, under feeding and drinking control: they were daily weighed and food and water consumption were measured.

Creation of skin wounds and treatment with 3D chitosan scaffolds

Three days before wounding, the dorsal interscapular area of each rat was depilated by a shaver and epilatory cream. The day of wounding the rats were anaesthetized by intraperitoneal injection of 50 mg/kg ketamine and 5mg/kg xylazine. Operative area of skin was cleaned with chlorhexidine. A punch biopsy instrument (diameter 8mm) was used to create two full-thickness round wounds in the interscapular region of the upper back of each rat, and the skin flap was excised by using iris scissors. During the procedure particular attention has been placed to avoid incision of the muscle layer. Rats were randomly assigned to two groups: Group 1 (n=13), with one wound covered with the 3D chitosan scaffold and the other one with a commercial product (positive control), Group 2 (n =12) with one wound covered with the 3D chitosan scaffold and the other one bare (negative control). The wounds were additionally covered with dry cotton gauze and with adhesive film as a secondary dressing. All dressings were fixed with an elastic adhesive bandage. The rats were singularly housed in large raised bottom mesh cages with free mobility. In the first week after the surgical procedure animals daily received paracetamol (100 mg/kg) in drinking water in order to prevent discomfort and pain.

Wound closure evaluation

After 7 or 14 days animals were sacrificed by CO₂ inhalation. The degree of wound healing was determined measuring the area of the wound with respect to a ruler by means of Image J software (<https://imagej.nih.gov/ij/index.html>) on photos of wounds taken at sacrifice.

After animal sacrifice, samples were excised from the area of the wound and immediately fixed in PBS-buffered paraformaldehyde at pH 7.4. Samples were then embedded in paraffin for sectioning using a microtome; slices of 6 μ m were cut and stained with hematoxylin-eosin, with the addition of sirius red to put into evidence collagen distribution. Images were taken using an optical microscope Nikon Eclipse 80i, equipped with a camera Nikon Digital Sight DS-2Mv and connected to the control software, NIS Elements F (Nikon Instruments, Italy).

Statistical Analysis

Results were expressed as mean \pm standard deviation (SD). One-way analysis of variation (ANOVA) was used for comparison of the experimental groups to a control group. A value of $p < 0.05$ was considered statistically significant.

RESULTS AND DISCUSSION

Preparation of 3D printed chitosan-based scaffolds and cell adhesion study

In order to properly evaluate, through qualitative and quantitative analysis, the formation of multi-layered, high-density cell populations in 3D scaffolds a highly reproducible and defined 3D printing process should be used. The preparation and characterization of the 3D printed scaffolds employed in this study was described by Elviri *et al.* [36] These scaffolds were characterized by an accurate geometry and good surface homogeneity in terms of pore size and distribution: on the surface of the filaments the pores (Feret diameter: $3.5 \pm 3 \mu\text{m}$) presented a preferential orientation, whereas regular interconnected and layered pore structure (Feret diameter: $5 \pm 4 \mu\text{m}$) within the filaments, were observed by SEM analysis. [19] Whereas the scaffold dehydration process causes a reduction in its size of about 45%, pore size ranges from 4 to 9 μm which could be beneficial for cell adhesion and migration.

As described in Materials & Methods section, mechanical resistance of scaffolds was measured with the help of a tensile tester. Young's modulus was calculated and resulted $105 \text{ kPa} \pm 18 \text{ kPa}$ ($n=6$). As reported by Liang and Boppart, [37] these values of elastic moduli are comparable to those observed in skin, in particular in volar forearm region. This suggests that if applied as wound healing patch, this could be integrated into wound and adapt to it.

All further experiments herein described were carried out using 3D printed chitosan-scaffolds patterned with a 200 μm geometry with and without a chitosan film at the bottom (Figure 1 A-B).

Keratinocyte visualization by optic light or scanning electron microscope microscopy on the 3D scaffolds from the bottom to the top was easier than that of fibroblasts, due to the geometry of these cells. Keratinocytes appeared as a ball with a rounded shape (Figure 2A) possessing a diameter of approximately 20 μm , in agreement with the literature [38]. Fibroblast, on the other hand, appeared elongated (about 50-100 μm length) and extremely thin, and for this reason were harder to visualize (Figure 2B). Moreover, all neutral red and scanning electron microphotographs posted in this work were collected and scanned from the top to the bottom part of the 3D scaffold. Only figures 8-10 were taken starting from the bottom side of the structures.

By testing 3D chitosan scaffold without and with a film of chitosan at the scaffold bottom, it was possible to provide evidences of how fibroblast and keratinocyte cells were able to attach, live and grow after 20 days (Figure 3). All parts of the scaffolds, on the filaments, inside the holes and on the planar substrate, seemed to be biocompatible with no toxicity observed towards the analyzed cell's phenotypes and appeared to be suitable to support colonization. These results indicated that the tested chitosan hydrogel was a suitable substrate for cell growth, in agreement with previous findings by Galli *et al.* [22] and Bettini *et al.* [18]. Furthermore, Figure 4 displays how the cells were able not only to grow on the structures, but also to fill the holes from the bottom to the top part of the scaffold trying to colonize the whole substrate. The best colonized scaffolds were observed with HaCaT cells seeded alone and analyzed after 20 days (Figure 3, 4), as well as with Nhdf and HaCaT cells together after 35 days, in both cases on the 3D chitosan scaffolds with the film at the bottom (Figure 5). In Figures 4 and 5, it was evident how the cells filled partially or completely the top part of the film and the walls of the holes. We hypothesize that HaCaT and Nhdf cells seeded together exhibited the best situation given their widely proved ability to collaborate each other releasing useful growth's factor for improving growth and vitality [38]. Moreover, at this stage, it was also visibly appreciable how the presence of the film on the base of the 3D structure resulted in a significant improvement in keeping the cells inside the scaffold (Figure 3, 4). This assumption was later confirmed by a proper analysis as shown in Figure 6. Further, a slower fibroblast growth appeared than that of keratinocytes

by Neutral Red analysis. This can be clearly seen in Figure 3 depicting Nhdf and HaCaT cells, taken at the 20 day time point after individual seeding. This finding was taken into consideration for setting up the next experiment where a higher starting number of fibroblast with respect to keratinocytes cells was used.

Cell viability analysis

Cell viability was evaluated by measuring the activity of the mitochondrial enzyme succinate dehydrogenase by MTT test as previously described. [39] Only the best experimental condition obtained by the Neutral Red analysis, namely, fibroblast (Nhdf) and keratinocyte (HaCaT) seeded together on 3D chitosan scaffold, was evaluated. The MTT assay confirmed the neutral red assay results showing how the chitosan substrate was not cytotoxic and that the cells were viable and able to grow and colonize 3D chitosan matrices. The graph in Figure 6 displays a significant presence and a steady increase of metabolically active cells on 3D chitosan scaffolds analyzed between 2 and 35 days for both structures without (2-35 days +38%; $p < 0.001$) and with film (2-35 days +16%; $p < 0.001$) (3D chitosan scaffolds without film percentage increase: 2-13 days +18%; 13-20 days +13%; 20-35 days +3%) (3D chitosan scaffolds with film percentage increase: 2-13 days +1%; 13-20 days +5%; 20-35 days +9%). Furthermore, it is worthy highlighting that the amount of metabolically active cells on the scaffolds with film was significantly higher than without at every time point sampled, as hypothesized above. These data clearly suggest how cell colonization on 3D chitosan scaffold with a film at the bottom can be significantly improved by this addition (percentage increase: 2 days +88%, $p < 0.01$; 13 days +62% $p < 0.0001$; 20 days +50% $p < 0.0001$; 35 days +58% $p < 0.0001$). Anyway, further considerations should be taken into account since 3D scaffolds with film kept higher number of cells on the structures but after 2 days a lower cell growth was measured in comparison with the structures without film. Instead, the graph in Figure 7 shows the comparison of cell growth between 2D and 3D structures and demonstrates how cells exploit the advantages of more complex constructs. The total amount of metabolic active cells adhered on the 3D scaffolds or located at the bottom of the

well where they came from was measured and represented on the graph. After 13 days in the 2D environment the cells reached the maximum confluence inhibiting cell growth, and remained almost constant during the later time points (13-20 days -2%; 20-35 days +2%). Contrariwise on the 3D substrate, the cell growth continued until 35 days for both experimental conditions assessed (3D chitosan scaffolds without film: 13-20 days +10%; 20-35 days +12%) (3D chitosan scaffold with film: 13-20 days +19%; 20-35 days +27%) even though the amount of active cells after 13 and 20 days was lower than that measured on the 2D configuration (Figure 7). The rate of 3D growth is slower due to the 3D scaffold surface topography which may reduce cell-to-cell signaling as cells are not interconnected in a single monolayer as they are in the 2D system. Therefore, although there is a higher surface availability in 3D the cell growth in first instance seems to be decelerated. We believe that the cells required a greater timeframe to adapt themselves to a much less regular matrice if compared to a plastic well-plate surface.

To confirm of our assumption, after 35 days the total number of metabolically active cells in to the 3D environments was comparable (3D scaffolds without film: 13 days -24% $p < 0.0001$; 20 days -15% $p < 0.01$; 35 days -7% $p < 0.05$) or higher (3D scaffolds with film: 13 days -28% $p < 0.0001$; 20 days -12% $p < 0.05$; 35 days +10% $p < 0.01$) with respect to the corresponding value to 2D at the same time point. These results demonstrated that in both conditions the 3D environment positively stimulated cell colonization and growth. Again, 3D chitosan scaffold with film seeded with both cell's phenotypes afforded the better results. This finding was also supported by SEM microphotographs (Figure 9). From these we hypothesize that the sugar-laden 3D chitosan scaffolds could possibly provide an additional carbon source of growth for the cells as the scaffold biodegrades. In fact, scaffolds appeared partially damaged and degraded when compared to the scaffolds without cells control (Figure 8).

Furthermore, the graph in Figure 6, shows a slight increase in optical density values of the cultured scaffold relative to 3D scaffold without cells after 20 and 35 days (+1 fold and +3 fold to 3D chitosan scaffolds without and with film). This supports the previous hypothesis, as this increase could be

ascribed to the absorbance of the oligosaccharides stemming from the chitosan degradation.

SEM analysis

Scanning electron microphotographs confirmed the successful colonization of the 3D structures.

Again, the best results appeared to be those obtained with Nhdf and HaCaT cells seeded together on 3D chitosan scaffold printed with the film at the bottom. Figure 9, clearly shows the difference of colonization on the 3D structures in 20 and 35 days. In particular, after 20 days only a few clusters of cells were spread on the surface areas of 3D scaffolds, whereas after 35 days the cells had filled the scaffolds and closed the gap between the previous clusters, reinforcing scaffold biocompatibility (Figure 9B-C). In addition, Figure 10, which displays images captured from the bottom side of the structures without film, shows how the cells were able to build and develop an early skin-like layer, consisting of a mass of fibroblast and keratinocyte cells growing together. The lower surface of the scaffolds was completely covered by both cell's phenotypes that in some cases were organized in several areas resembling a protruding cluster or filopodia (Figure 10).

In-vivo test

Starting from a wound having area of about 0,5 cm², after seven days both treatments and negative control lead to a general reduction of wound area, with a high variability among animals and with a more consistent, although not significant ($p>0.05$) reduction in wounds treated with the commercial product. After 14 days, untreated wounds still showed a scab (wound area $0.025 \pm 0,001$ cm²), while wounds treated were almost completely healed and only scars were visible (chitosan scaffold treatment: wound area $0.005 \pm 0,002$ cm²; positive control treatment: wound area $0.004 \pm 0,001$ cm²). On the whole, visual inspection of wound confirmed that treatment improved and accelerated wound healing with respect to untreated animals, but did not show significant differences between wounds treated with chitosan scaffolds with respect to commercial product. On the other hand some

differences in the quality of wound healing could be appreciated by histological analysis. Figure 11 shows the comparison of a wound treated with chitosan hydrogel (left) with respect to spontaneous healing (right), 7 days after wound infliction. The scarlet area on the side of both images marks the limit of original wound, evidencing collagen structure. In figure on the left, the intense purplish red area is indicative of a more intense tissue reorganization, with respect to the pale pink area of the photo on the right, where tissue organization and collagen is very scarce. Epidermis is present only in the wound treated with chitosan hydrogel. In both images, healing is still ongoing, but the tissue formed on the wound treated with chitosan scaffold has a more mature appearance.

Figure 12 shows the comparison of a wound treated with chitosan hydrogel (left) with respect to a commercial product (right), 14 days after wound infliction. On the left, it is not possible anymore to distinguish the site of wound infliction, since the tissue is completely reorganized and the epidermis repaired (purple layer up), with a huge amount of collagen (scarlet red) into which tissue annexes are present such as blood vessels (v), sebaceous glands (g), hair follicles (h) and erector pili muscles (p). On the other hand, figure on the right shows a wound treated with the commercial product: resulting tissue shows a non-ordered distribution of collagen that surrounds an area of tissue, that appears like fat tissue, with a functionality that is still compromised and no evidence of tissue annexes.

CONCLUSIONS

3D chitosan bio-polymeric scaffolds were fabricated using a newly developed extrusion-based 3D printing technique. This system provided a tool for precisely controlling the final shape and spatial distribution of the 3D chitosan structures.

These scaffolds exhibit excellent properties in terms of biocompatibility, cytocompatibility and toxicity toward two different skin associated human cell lines, namely Nhdf and HaCaT. These cell lines successfully attached, grew, and colonized the 3D structures. The best results were obtained when the two cell lines were seeded together onto 3D chitosan scaffolds with chitosan films at the base. Proliferating cells adhere and spread on the chitosan scaffold where interconnected cells form

a continuous layer, which is significant for potential application in skin integrity restoration. Moreover *in vivo* tests on rat models of diabetes showed that the use of chitosan scaffolds to treat wounds leads to a reduction in the time of healing with respect to untreated ones and promotes the regeneration of a tissue with an improved functionality with respect to wounds treated with a commercial product, suggesting the usefulness of chitosan scaffolds for the treatment of chronic dermal wounds.

REFERENCES

- 1 Khademhosseini A, Vacanti JP, Langer R. Progress in tissue engineering. *Sci A* 2009;**300**:64–71.
- 2 Yannas IV, Lee E, Orgill DP, Skrabut EM, Murphy GF. Synthesis and characterization of a model extracellular matrix that induces partial regeneration of adult mammalian skin. *PNAS* 1989;**86**:933-937.
- 3 Atala A, Bauer SB, Soker S, Yoo JJ, Retik AB. Tissue-engineered autologous bladders for patients needing cystoplasty. *Lancet* 2006;**367**:1241-6.
- 4 Macchiarini P. Clinical transplantation of a tissue-engineered airway *Lancet* 2008;**372**: 2023-30.
- 5 Schimming R, Schmelzeisen R. Tissue-engineered bone for maxillary sinus augmentation. *J Oral Maxillofac Surg* 2004;**62**:724-9.
- 6 Warnke PH Growth and transplantation of a custom vascularised bone graft in a man. *Lancet* 2004;**364**:766-70.
- 7 Zhang X, Liu Z, Yang Y, Yao Y, Tao Y. The clinical outcomes of vaginoplasty using tissue-engineered biomaterial mesh in patients with Mayer-Rokitansky-Küster-Hauser syndrome. *International J Surgery* 2017;**44**:9-14.

- 8 Chen KL, Wu HC, Chang CH. Tissue-engineered constructs for urethral regeneration. *Urological Sci* 2012;**23**:42-44.
- 9 Bello YM, Falabella AF, Eaglstein WH. Tissue-Engineered Skin. *American Journal of Clinical Dermatol* 2001;**2**:305-313.
- 10 Xue M, Jackson CJ. Extracellular Matrix Reorganization During Wound Healing and Its Impact on Abnormal Scarring. *Adv Wound Care* 2015;**4**:119–136.
- 11 Ho MH, Kuo PY, Hsieh HJ, Hsien TY, Hou LT, Lai JY, Wang DM. Preparation of porous scaffolds by using freeze-extraction and freeze-gelation methods. *Biomater* 2004;**25**:129-38.
- 12 Weigel T, Schinkel G, Lendlein A. Design and preparation of polymeric scaffolds for tissue engineering. *Expert Rev Med Devices* 2006;**3**:835-51.
- 13 Ko YG, Oh HH, Kawazoe N, Tateishi T, Chen G. Preparation of Open Porous Hyaluronic Acid Scaffolds for Tissue Engineering Using the Ice Particulate Template Method. *J Biomater Sci Polym* 2011;**22**:123-38.
- 14 Azhari A, Toyserkani E, Villain C. Additive manufacturing of graphene–hydroxyapatite nanocomposite structures. *Int J Appl Ceramic Technol* 2015;**12**:8-17.
- 15 Karande TS, Ong JL, Agrawal CM. Diffusion in musculoskeletal tissue engineering scaffolds: design issues related to porosity, permeability, architecture, and nutrient mixing. *Ann Biomed Eng* 2004;**32**:1728-43.
- 16 Stevens MM, George JH. Exploring and engineering the cell surface interface. *Science* 2005;**310**:1135–1138.
- 17 Arslan-Yildiz A, El Assal R, Chen P, Guven S, Inci F, Demirci U. Towards artificial tissue models: past, present, and future of 3D bioprinting. *Biofabrication* 2016;**8**:1-8.
- 18 Bettini R, Romani AA, Morganti MM, Borghetti AF. Physicochemical and cell adhesion properties of chitosan films prepared from sugar and phosphate-containing solutions. *Eur J Pharm Biopharm* 2008;**68**:74-81.
- 19 Elviri L, Foresti R, Bergonzi C, Zimetti F, Marchi C, Bianchera A, Bernini F, Silvestri M,

- Bettini R. Highly defined 3D printed chitosan scaffolds featuring improved cell growth. *Biomed Mater* 2017;**12**: 045009.
- 20 Elviri L, Asadzadeh M, Cucinelli R, Bianchera A, Bettini R. Macroporous chitosan hydrogels: Effect of sulfur on the loading and release behaviour of amino-acid based compounds. *Carbohy Polym* 2014;**132**:50-58.
- 21 Gasperini L, Mano JF, Reis RL. Natural polymers for the microencapsulation of cells. *J. R. Soc. Interface.* 2014;**11**: 20140817.
- 22 Galli C, Parisi L, Elviri L, Bianchera A, Smerieri A, Lagonegro P, Lumetti S, Manfredi E, Bettini R, Macaluso GM. Chitosan scaffold modified with D-(+) raffinose and enriched with thiol-modified gelatin for improved osteoblast adhesion. *Biomed Mater* 2016;**11**: 015004.
- 23 Patil RS, Ghormade VV, Deshpande MV. Chitinolytic enzymes: an exploration. *Enzyme Microb Technol* 2000;**26**:473–83.
- 24 Kumar MN, Muzzarelli RA, Muzzarelli C, Sashiwa H, Domb AJ. Chitosan chemistry and pharmaceutical perspectives. *Chem Rev* 2004;**104**:6017–84.
- 25 Peluso G, Petillo O, Ranieri M, Santin M, Ambrosio L, Calabro D, Avallone B, Balsamo G. Chitosan-mediated stimulation of macrophage function. *Biomaterials* 1994;**15**:1215-20.
- 26 Okamoto Y, Minami S, Matsushashi A, Saimoto H, Shigemasa Y, Tanigawa T, Tanaka Y, Tokura S. *Advances in chitin and chitosan* Elsevier: New York, 1992.p. 70.
- 27 Ueno H, Yamada H, Tanaka I, Kaba N, Matsuura M, Okumura M, Kadosawa T, Fujinaga T. Accelerating effects of chitosan for healing at early phase of experimental open wound in dogs. *Biomaterials* 1999;**20**:1407–14.
- 28 Mizuno K, Yamamura K, Yano K, Osada T, Saeki S, Takimoto N, Sakura T, Nimura Y. Effect of chitosan film containing basic fibroblast growth factor on wound healing in genetically diabetic mice. *J Biomed Mater Res* 2003;**64**:177–81.
- 29 Ahn JS, Choi HK, Cho CS. A novel mucoadhesive polymer prepared by template

- polymerization of acrylic acid in the presence of chitosan. *Biomaterials* 2001;**22**:923–8.
- 30 Ahn JS, Choi HK, Chun MK, Ryu JM, Jung JH, Kim YU, Cho CS. Release of triamcinolone acetonide from mucoadhesive polymer composed of chitosan and poly (acrylic acid) in vitro. *Biomaterials* 2002;**23**:1411–6.
- 31 Zhao F, Yin Y, Lu WW, Leong JC, Zhang W, Zhang J, Zhang M, Yao K. Preparation and histological evaluation of biomimetic three-dimensional hydroxyapatite/chitosan–gelatin network composite scaffolds. *Biomaterials* 2002;**23**:3227–34.
- 32 Teng YD Lavik EB, Qu X, Park KI, Ourednik J, Zurakowski D, Langer R, Snyder EY.. Functional recovery following traumatic spinal cord injury mediated by a unique polymer scaffold seeded with neural stem cells. *Proc Natl Acad Sci USA* 2002;**99**:3024–3029.
- 33 Mekhail M, Tabrizian M. Injectable chitosan-based scaffolds in regenerative medicine and their clinical translatability. *Adv Healthc Mater.* 2014;**10**:1529-45.
- 34 Alvatex® Simple Visualisation of Cells on Alvatex® Scaffold Using Light Microscopy *Amsbio.*
- 35 Alvatex® MTT cell viability assay of cultures grown on alvatex® in 3D *Amsbio.*
- 36 Elviri L, Bianchera A, Bergonzi C, Bettini R. Controlled local drug delivery strategies from chitosan hydrogels for wound healing. *Exp Opin Drug Deliv* 2016;**14**:897-908.
- 37 Liang X, Boppart SA, Biomechanical Properties of In Vivo Human Skin From Dynamic Optical Coherence Elastography. *IEEE Trans Biomed Eng* 2010;**57**:953–959.
- 38 Barrandon Y and Green H. Cell size as a determinant of the clone-forming ability of human keratinocytes. *PNAS* 1985;**82**:5390-5394.
- 39 Favari E, Zanotti I, Zimetti F, Ronda N, Bernini F, Rotblath GH. Probucol inhibits ABCA1-mediated cellular lipid efflux. *Arterioscler Thromb Vasc Biol* 2004;**24**:2345-2350.

